

Title: The complex coupling of shape and hydrodynamic forces in the collisions and coalescence of bubbles

Ivan U. Vakarelski^{1,2,3}, Rogerio Manica⁴, Raymond R. Dagastine^{1,2}, Xiaosong Tang⁵, Sean J. O'Shea⁵, Geoffrey W. Stevens^{1,2}, Franz Grieser^{1,6}, Derek Y. C. Chan^{1,7,8 *}

¹Particulate Fluids Processing Centre, The University of Melbourne, Victoria 3010 Australia.

²Department of Chemical and Biomolecular Engineering, The University of Melbourne, Victoria 3010 Australia.

³Institute of Chemical and Engineering Sciences, 1 Pesek Road, Jurong Island, 627833 Singapore

⁴Institute of High Performance Computing, 1 Fusionopolis Way, 138632 Singapore

⁵Institute of Materials Research and Engineering, 3 Research Link, 117602 Singapore

⁶School of Chemistry, The University of Melbourne, Victoria 3010 Australia.

⁷Department of Mathematics and Statistics, The University of Melbourne, Victoria 3010 Australia.

⁸Department of Mathematics, National University of Singapore, 117543 Singapore.

* Author to whom correspondences should be addressed:

Derek Chan
Department of Mathematics and Statistics
University of Melbourne
Victoria, 3010 Australia
Email: D.Chan@unimelb.edu.au
Ph: 61-3-8344 5556
Fax: 61-3-8344 4599

Abstract

We report direct measurements and quantitative modelling of micro-bubble collisions that demonstrate a counter-intuitive coalescence on separation phenomenon that is a consequence of the interplay between van der Waals-Lifshitz attraction, hydrodynamic drainage effects and dynamic bubble deformability. The combined dynamic effects and deformations cause a bubble pair to be more stable at higher approach velocities, and to coalesce when pulled apart or when suddenly halted. We also demonstrate that fluctuations in the water film thickness play no role in bubble coalescence.

PACS numbers: 47.55.D-, 47.55.dd, 47.55.df, 47.57.Bc

Bubble coalescence is a complex multi-length scale process where studies have focused on bubble size ranges from centimetres to nanometres in order to gain a fundamental understanding of the phenomenon that underpins a range of processes, from foam stability in minerals processing to the design of ultrasonic contrast agents [1]. Based on a number of studies a complicated picture of bubble behaviour has emerged, but there tends to be consensus on two aspects. First, the coalescence events are governed by dynamic interactions on the scale of nanometres [2]. Second, the direct observation of these events coupled to a quantitative physical model on the scale of nanometres has proven elusive [1, 3]. This is due to that fact that both bubbles and droplets offer more complex and interesting behaviour compared to that between rigid materials because of the coupling between the geometry of deformation to their dynamic interaction forces. For micron sized droplets, observations of the importance of this coupling between have begun to come into focus, where examples include, long-ranged velocity-dependent attractive forces observed between separating deformable emulsion droplets in water [4], the initial thinning of the nanometre thick water film between a mercury droplet and a solid surface upon the initiation of separation [5], the triggering of coalescence between proximal drops in a four-roll mill [6] and in microfluidic devices [7].

The interaction between bubbles provides simplest model system to study the coupling between forces and deformations that defines the dynamic interaction between soft matter (bubbles, drops, emulsions, biological cells, soft tissues and gels) albeit more difficult to extract quantitative measurements on the nanoscale. We report direct measurements of accurately controlled collision experiments between two deformable micro-bubbles in water under conditions where only attractive van der Waals-Lifshitz forces and hydrodynamic interactions together with bubble deformations determine whether each collision event results in bubble stability or coalescence. The observed behaviour can be counter-intuitive to expectation developed from studying collisions between rigid particles. The well-defined experimental conditions also provide the basis for precise theoretical modelling to elucidate the complex time-dependent interactions that arise from the coupling between forces and geometric deformations. Agreement between experiment and theory indicate that the no-slip hydrodynamic boundary condition applies at the bubble surface in our system. The model is also used to demonstrate that thermally excited fluctuations in the thickness of the water film between the bubbles, which for

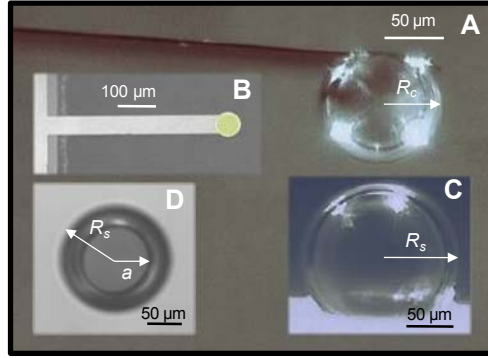


Fig. 1. (A) Side view of the bubble anchored on the tip of the cantilever. (B) Plan view of the custom made cantilever with the hydrophobised circular anchor pad for the bubble. (C) Side perspective of the bubble on the substrate. (D) Bottom view of the bubble showing the dark circular contact zone (in focus) on the substrate and the bubble diameter.

decades was regarded as the key step in film rupture[2], plays no role in the present coalescence experiments. In soft matter systems, the dynamic coupling between forces and deformations is a critical element that should be incorporated in general intuitive considerations of the material properties such systems.

We use an atomic force microscope to produce precisely controlled single collision events between two micro-bubbles [8]: one positioned on a planar substrate and the other anchored at one end of a custom-fabricated microcantilever (Fig. 1A–D). To initiate the collision, the other end of the cantilever is first moved towards (“approach”) and then away (“retract”) from the planar substrate by a piezo-electric transducer whose displacement $X(t)$ is varied accurately with time, t by a linear variable differential transformer (Fig. 1E) and actual values of $X(t)$ are used in all subsequent modelling. The maximum piezo-electric motor displacement is in the range 1.5–6 μm and average speeds are 50–80 $\mu\text{m/s}$. The time-dependent force between the colliding bubbles is obtained from the cantilever deflection, measured with a reflected laser beam.

Working at a salt concentration close to that of seawater or hypertonic saline (0.5 M NaNO_3) that would completely suppress electrical double layer repulsion between the bubbles, the physical forces that can affect bubble coalescence are: (i) surface tension force that minimises the surface area of the deformable bubbles as described by the Young-Laplace theory [9], (ii) attractive van der Waals-Lifshitz force [10, 11] (including effects due to electromagnetic

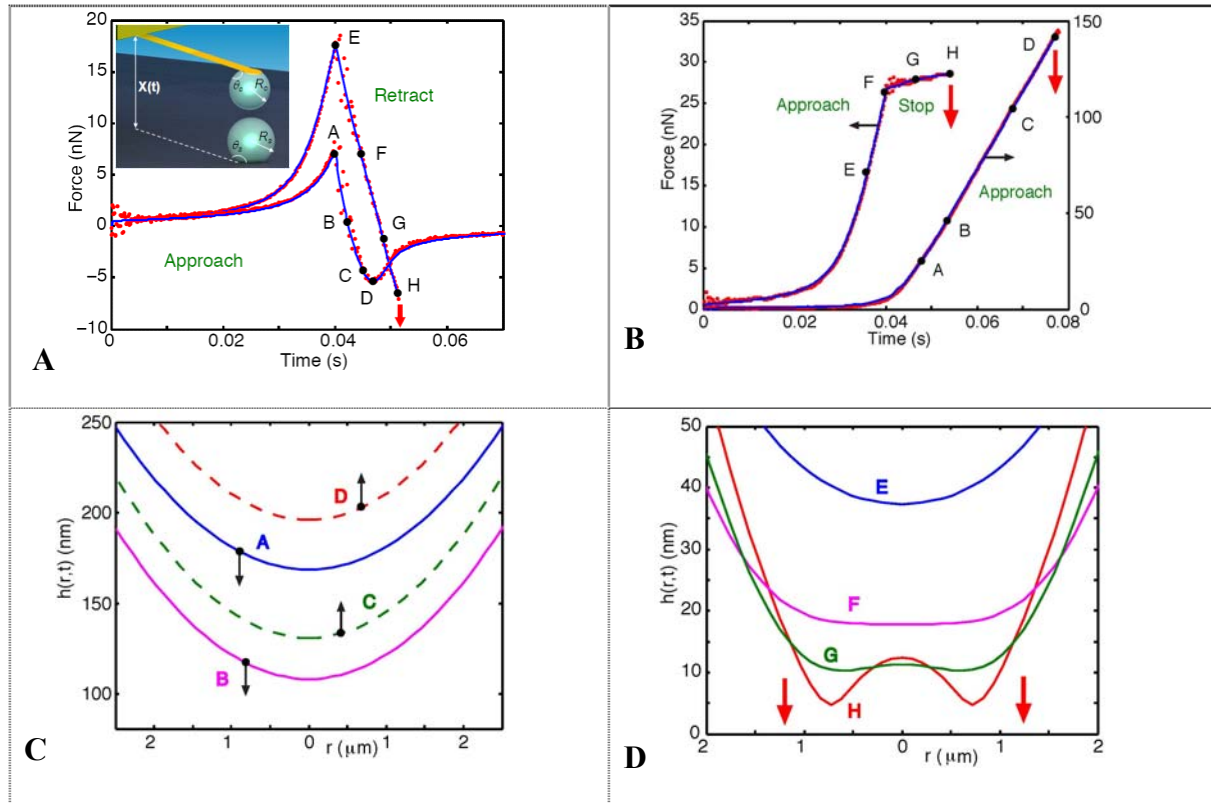


Fig. 2. (A) Forces between the two identical bubbles (radii $74 \mu\text{m}$) colliding during an approach-retract cycle at nominal speed $50 \mu\text{m/s}$. Curve A-D is first measured with initial separation $h_o = 2.45 \mu\text{m}$ and then curve E-H with $h_o = 2.45 \mu\text{m}$. Coalescence is indicated by the arrow at time H. Points are measurements and continuous lines are theoretical predictions. **Inset:** Schematic representation of the interacting bubbles with their contact angles. (B) Forces between two bubbles prior to coalescence under continual approach (right axis, bubble radii 62 and $86 \mu\text{m}$, $h_o = 5.50 \mu\text{m}$) or approach-stop (left axis, bubble radii 67 and $85 \mu\text{m}$, $h_o = 1.65 \mu\text{m}$) conditions. (C) Calculated water film thickness $h(r,t)$ of the stable collision (curve A-D of (A)) during the retraction phase with solid (broken) lines indicating decreasing (increasing) film thickness. (D) Calculated water film thickness during separation in the retraction phase (curve E-H of (A)) leading up to coalescence indicated by arrows.

retardation) between the bubbles and (iii) hydrodynamic force generated by relative bubble motion and the associated flow of water, where Reynolds lubrication theory [12] for flow in thin films gives a good description. A theoretical model that encompasses all these features [13] with the latest dielectric data for water [14] to calculate van der Waals-Lifshitz forces is used to analyse our measurements.

Examples of different collision outcomes from about 100 collision experiments are given in Fig. 2. In all cases, the bubbles are initially undeformed and stationary at a distance of closest approach h_o in the range $1-6 \mu\text{m}$. The cantilever-substrate separation $X(t)$ is then decreased by an

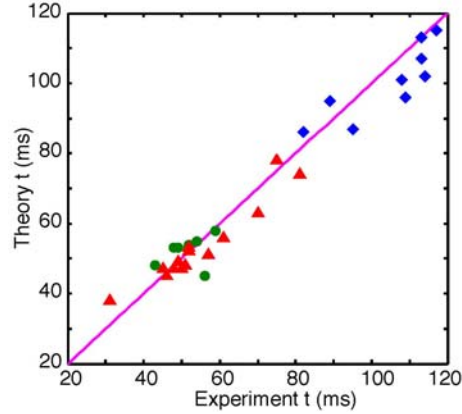


Fig. 3. A comparison of experimental and theoretical coalescence times are measured from the start of the approach phase for coalescence-on-separation (red triangles), coalescence-on-approach (blue diamonds) and coalescence on stopping of the piezo drive after approach (green circles) from 30 measurements.

amount that would ensure the bubbles are driven together beyond the point where they will come into contact if they were not to deform. The time-dependent force $F(t)$ curves during collision between two consecutive measurements on the same bubble pair (identical radii $74 \mu\text{m}$) but from different initial separations are shown in Fig. 2A. Since the van der Waals-Lifshitz force is attractive, the repulsive dynamic force on approach is due solely to hydrodynamic interactions, as water has to be displaced between the approaching bubbles. For the same distance traversed by the piezo drive, the magnitude of the repulsive force maximum is determined by the initial separation, h_o . The continuous lines are predictions of the theoretical model with a fitted value of h_o which is within the estimated experimental range. At $h_o = 2.45 \mu\text{m}$, the force becomes attractive during the retraction phase but the bubbles do not coalesce and ultimately separate. This attraction is again of hydrodynamic origin as water has to be drawn into the gap between the separating bubbles. For a repeat run with the same bubble pair starting closer at $h_o = 2.05 \mu\text{m}$, the magnitude of the repulsion on approach is higher because the bubbles are now driven closer together, resulting in larger deformations. As the bubbles undergo separation, coalescence occurs at the time predicted by theory near the attractive force minimum (point H marked by the down arrow in Fig. 2A).

The no-slip or immobile interface hydrodynamic boundary condition at the bubble surface is required to give the excellent agreement between experiment and theory. The fully mobile or no tangential stress boundary condition, normally assumed to hold at the air/water interface,

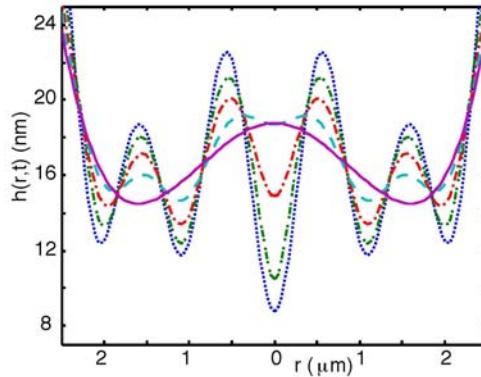


Fig. 4. An undulating perturbation is imposed on the film at time G in Fig. 2d and is allowed to evolve. The time intervals between successive profiles, starting from the initial perturbed film given by the dotted (blue) line are: 2, 2, 4, and 40×10^{-5} seconds. The final film profile is indistinguishable from the initial unperturbed film profile (continuous purple curve) as the film thickness did not change appreciably during the short time it took for the imposed perturbation to be damped out.

cannot predict the magnitudes of the dynamic force or the coalescence time. Although experiments with rising bubbles [15] show that very rigorous cleaning of ultra-pure water appears to produce the fully mobile boundary condition, this regime, if it can be realised in our experiment, will have little relevance to behaviour under real operating environments [16]. Dynamic effects of surface-active agents at a surface concentration that reduces the interfacial tension by ~ 1 mN/m would suffice to cause bubbles to exhibit the no-slip boundary condition [17, 18].

In Fig. 2B, we show the two bubbles driven under different conditions. In one case (curve A–D, bubble radii 62 and 86 μm , $h_o = 5.50$ μm), they are driven much closer together to give a force that is about 8 times larger than that in Fig. 2A, whence they coalesce on approach. In the other case in Fig. 2B (curve A–D, bubble radii 67 and 85 μm , $h_o = 1.65$ μm), the bubbles are driven together to a moderate repulsive force of about twice that in Fig. 2A then the piezo drive is stopped rather than retracted. From this point on, the force between the bubbles remains approximately constant while the water film between the bubbles continues to thin, and coalescence occurs suddenly in the constant force region (Fig 2B curve F-H). This approach-stop protocol mimics the situation in foam films.

Given the quantitative success of the model, it can be used with confidence to predict the position and time variations of the thickness of the water film, $h(r,t)$ between the bubbles (see Fig. 1E for definition). Calculated film thickness of the central portion ($\sim 5 \mu\text{m}$) of the film between the two bubbles for the approach and retract without coalescence (Fig 2 A, curve A-d) are shown in Figs. 2C. When the film is at its thinnest for the stable case (curve B in Fig. 2B), the flattening of each bubble is estimated to be 35 nm at the centre, $r = 0$. The attractive force minimum (point D in Fig 2A and C) occurs when the film is actually increasing in thickness.

The behaviour for all three coalescence cases is similar (Fig 2A, curve E-H and Fig 2B): the central portion of the film (shown for approach-retract curve, Fig 2A, curve E-H in Fig. 2D) thins, flattens, forms a dimple and ultimately coalesces when the thinnest portion of the film located at the dimple radius becomes sufficiently thin for the attractive van der Waals-Lifshitz force to destabilise the film (indicated by arrows). What delineates these cases is when the film first flattens and forms the dimple with respect to the approach and retract phases of the piezo drive. For the coalesce on separation case (Fig 2D), the interfacial flattening occurs well into the retract phase and dimple formation appears close to the coalescence point. For the continual approach curve (Fig 2B, curve A-d), the water film between the bubbles forms a hydrodynamic dimple during the approach phase (Fig. 2D) and coalesces before the commencement of the retraction phase [19]. For the approach-stop case, coalescence occurs in the constant force region (Fig 2B curve E-H)[19].

The excellent agreement between observed and predicted coalescence times (Fig. 3) for the two different drive modes of dynamic bubble interaction (approach-retract or approach-stop) collected from 30 coalescence experiments is very strong evidence that the coalescence time can be predicted accurately and that coalescence occurs when the film at the dimple rim becomes thin enough to be within the range of van der Waals-Lifshitz attraction, irrespective of whether the bubbles are approaching or separating.

What then is the role of thermally excited surface fluctuations that are postulated in the long accepted model of coalescence [2]? We use our theoretical model to elucidate the stability of the thinning water film between two bubbles due to perturbations arising from fluctuations in

thickness. Starting with the film at time G in Fig. 2D, we impose an undulating perturbation that changes the local film thickness by over 50% and then follow how the film will evolve. We see in Fig. 4 that the initially perturbed film (dotted line) returns to its former shape (solid line) in around 10^{-4} s, which is significantly shorter than the time of 10^{-2} s required for the film to evolve from time G to H in Fig. 2D. Even though the imposed perturbation is extremely large, its rapid dampening demonstrates clearly that surface fluctuations are very short-lived according to the model that has already been shown to predict dynamic behaviour of the micro-bubbles with high precision. Therefore the long accepted conjecture that coalescence takes place via thermal fluctuations [2] appears to play no role in the present well-controlled study of dynamic micro-bubble coalescence.

Through detailed measurements and accurate modelling we demonstrate unambiguously that under dynamic conditions, when hydrodynamic effects and bubble deformations play a key role, there exist two dynamic modes of bubble coalescence – as the bubbles approach or counter-intuitively, as they separate. Unless driven together under high forces, coalescence-on-separation is likely to be the mechanism whereby the water film between the bubbles at the dimple ring can become sufficiently thin for attractive van der Waals-Lifshitz forces to destabilise the film. Furthermore, the coalescence time is a predictable quantity and does not involve the long accepted conjecture of coalescence being triggered by thermally excited surface waves. Such fluctuations are shown to damp out very rapidly on the characteristic time scale of the film thinning process.

The rich and complex time-dependent dynamic interactions in the present simple system of two interacting bubbles arise from the coupling of well-defined primary forces due to van der Waals-Lifshitz attraction, hydrodynamic interactions and geometric deformations. The insight gained will inform analysis of interactions and the design of desired material properties that involve more complex soft matter systems such as drops, emulsions, foams, biological cells and soft tissues systems.

References

- [1] D. Lohse, *Phys. Today* **56**, 36 (2003).
- [2] I. B. Ivanov, *Thin Liquid Films* (Marcel Dekker, 1988).
- [3] A. Prosperetti, *Phys. Fluids* **16**, 1852 (2004).
- [4] R. R. Dagastine *et al.*, *Science* **313**, 210 (2006).
- [5] R. Manica *et al.*, *Langmuir* **24**, 1381 (2008).
- [6] L. G. Leal, *Phys. Fluids* **16**, 1833 (2004).
- [7] N. Bremond, A. R. Thiam, and J. Bibette, *Phys. Rev. Lett.* **100**, 024501/1 (2008).
- [8] I. U. Vakarelski *et al.*, *Langmuir* **24**, 603 (2008).
- [9] H. Lamb, *Statics, including hydrostatics and the elements of the theory of elasticity* (Cambridge University Press, 1928).
- [10] H. B. G. Casimir, *Proc. K. Ned. Akad. Wet.* **51**, 793 (1948).
- [11] I. E. Dzyaloshinskii, E. M. Lifshitz, and L. P. Pitaevskii, *Adv. Phys.* **10**, 165 (1961).
- [12] G. K. Batchelor, *An introduction to fluid dynamics* (Cambridge University Press, 1967).
- [13] R. Manica *et al.*, *Phys. Fluids* **20**, 032101/1 (2008).
- [14] R. R. Dagastine, D. C. Prieve, and L. R. White, *J. Colloid Interface Sci.* **231**, 351 (2000).
- [15] L. Parkinson *et al.*, *J. Colloid Interface Sci.* **322**, 168 (2008).
- [16] G. H. Kelsall *et al.*, *J. Chem. Soc. Faraday Trans.* **92**, 3879 (1996).
- [17] O. Manor *et al.*, *Langmuir* **24**, 11533 (2008).
- [18] O. Manor *et al.*, *Phys. Rev. Lett.* **101**, 024501/1 (2008).
- [19] See EPAPS Document No. [number will be inserted by publisher] for additional details on the methods, modelling, interfacial profiles and animated visualization of the results.
- [20] This work is supported in part by the Australian Research Council through funding of the Particulate Fluids Processing Centre and the Australian Minerals Science Research Institute.